

Effect of nominal substitution of transition metals for excess Fe in Fe_{1+x}Se superconductor

Anil K Yadav¹, Santosh Kumar¹, Anup V Sanchela¹, Ajay D Thakur², C V Tomy¹

¹ *Department of Physics, Indian Institute of Technology Bombay, Mumbai 400076, India*

² *School of Basic Sciences, Indian Institute of Technology Patna, Patna 800013, India*

Abstract

Taking cue from the increase in the superconducting transition temperature (T_c) of Fe_{1+x}Se via nominal (2 wt%) substitution of Cr instead of excess Fe, we have now extended our study with nominal substitution (≤ 5 wt%) with other transition metals (Ni, Co, Fe, Mn, Cr, V and Ti) in place of excess iron. The T_c is found to increase (maximum ~ 11 K) or get suppressed depending on the substituted transition metal. Our studies indicate that the superconducting transition temperature depends on various parameters like the ionic size of the transition metal, its magnetic moment as well as the amount of hexagonal phase present as impurity.

PACS numbers: 74.25.Ha, 74.62.Bf, 74.62.Dh, 74.70.Xa, 81.10.Fq.

I. INTRODUCTION

Discovery of superconductivity in $\text{LaFeAsO}_{1-x}\text{F}_x$ with a $T_c \sim 26$ K in 2008 [1] led to an outburst of research activity towards finding new Fe-based superconductors and increasing their T_c , which resulted in the identification of at least six family [1–7] of Fe-based superconductors with the highest T_c of ~ 56 K reported in $\text{Gd}_{0.8}\text{Th}_{0.2}\text{FeAsO}$ [8]. Among these superconductors, FeSe (Fe-11) based superconductors have the lowest T_c . Stoichiometric $\text{Fe}_{1.0}\text{Se}_{1.0}$ has a NiAs-type hexagonal (space group $P6_3/mmc$) crystal structure and does not exhibit superconductivity at ambient pressure. However, with a small excess of Fe at the Fe-site (Fe_{1+x}Se , $x \sim 0.01$), the crystal structure gets stabilized into a tetragonal structure (space group $P4/nmm$ space group) which shows superconductivity with a $T_c \sim 8.5$ K [4]. Even though the crystal structure of Fe-11 resembles that of the other pnictides superconductors, the structure is less complex and consists of only the alternate Fe–Se planes with no spacer layers in between, which makes them ideal materials to investigate the superconducting properties in Fe-based high T_c superconductors in general. Application of an external pressure is found to increase the T_c of the Fe-11 compounds [9–11]. Even for the non-superconducting stoichiometric compound $\text{Fe}_{1.0}\text{Se}_{1.0}$, superconductivity can be achieved with a T_c as high as 27 K with an applied pressure of $P = 1.48$ GPa [9]. The T_c of the non-stoichiometric tetragonal compound $\text{Fe}_{1.01}\text{Se}$ increases initially with the hydrostatic pressure, attaining a maximum T_c of ~ 37 K for $P \sim 7$ GPa and then decreases down to ~ 6 K at 14 GPa [10]. In all the pressure effect studies on T_c , it is found that the non-superconducting hexagonal phase increases along with the increase in T_c . As the crystal structure gets completely transformed into the hexagonal phase, superconductivity gets fully suppressed [11] implying that there is an optimum ratio between the two phases for the maximum T_c . The alternate way to increase T_c of the Fe-11 compounds is the chemical pressure, achieved by the doping of other chemical elements at the Fe or Se site. T_c is found to increase to a maximum of ~ 15 K at ambient pressure by substituting 50% Te at the Se site [12–15], whereas the S substitution at the Se site is found to increase T_c , only to a maximum of ~ 10.5 K [16]. Wu *et al.*, [17] have studied the effect of substitution (more than 10 %) at the Fe site by non transition metals (Al, Ga, In, Sm, Ba) and transition metals (Ti, V, Cr, Mn, Co, Ni and Cu) in the Fe_{1+x}Se compound, but could not observe any enhancement in T_c . The only other family of compounds which showed a maximum T_c of ~ 32 K amongst the FeSe-based compounds is the $A_x\text{Fe}_{2-y}\text{Se}_2$ ($A = \text{K, Cs, Rb}$) family of compounds, but with a different [18–20] crystal structure (ThCr_2Si_2 structure, space group $I4/mmm$). We have earlier reported an increase in T_c upto 11 K by substituting excess Cr (2%) at the Fe site, instead of excess Fe [21, 22]. This motivated us to investigate the effect of nominal substitution of other transition metal (TM) elements at the Fe site in the Fe_{1+x}Se

compound. The substitution of TMs was started with $x = 0.1$ and then subsequently increased to search for the optimal stoichiometry for the maximum T_c and diamagnetic shielding fraction in each substitution. In this paper, we present the physical properties (structural, magnetization, electrical transport and thermal transport) only for the optimally doped FeT_xSe , ($T = \text{Fe, Mn, Cr, V, Ti}$) compounds, which show the maximum T_c . We could not observe a clear evidence for superconductivity when Ni and Co was substituted in place of Fe. Our studies indicate that the superconducting transition temperature depends on various parameters like the ionic size of the transition metal, its magnetic moment as well as the amount of hexagonal phase present as impurity.

II. EXPERIMENTAL TECHNIQUES

Polycrystalline samples of FeT_xSe ($T = \text{Ni, Co, Fe, Mn, Cr, V}$ and Ti) were prepared via conventional solid state reaction method. The starting materials of high purity element powders were taken in stoichiometric ratio and mixed in an agate mortar. The mixture was then heated in an evacuated quartz tube at $20^\circ\text{C}/\text{hour}$ and held at 1050°C for 24 hours. After that, the samples were cooled slowly down to 360°C , held at that temperature for 24 hours and then quenched from this temperature in liquid nitrogen (LN2). The quenching process was adopted to minimize the formation of α -FeSe hexagonal phase, since the tetragonal β -phase is known to exist above $\sim 300^\circ\text{C}$ [23, 24]. For studying the effect of quenching, a few samples ($T = \text{Fe, Mn, Ti}$ and V) were also synthesized by cooling to room temperature in the final stage instead of quenching from 360°C . Powder X-Ray diffraction ($\text{Cu-K}\alpha$) patterns were obtained using a Panalytical X'Pert Pro (θ - 2θ scans) for the structural analysis and the phase purity determination. For the chemical identification and the stoichiometry analysis, the energy dispersive X-ray spectroscopy (EDAX) was performed. DC magnetization and ac susceptibility ($H_{ac} = 3.5 \text{ Oe}$ and frequency $f = 211 \text{ Hz}$) measurements were carried out in a Superconducting Quantum Interference Device - Vibrating Sample Magnetometer (SVSM) (Quantum Design, USA). Electrical resistance using four probe method was measured using the resistivity option of the Physical Property Measurement System (PPMS), Quantum Design Inc., USA. Thermal conductivity and thermopower measurements were performed via the thermal relaxation method in the TTO option of the PPMS.

III. RESULTS

A. Structure analysis

Typical room temperature X-ray powder diffraction patterns of FeT_xSe ($T = \text{Ni}, \text{Co}, \text{Fe}, \text{Mn}, \text{Cr}, \text{V}$ and Ti) samples for the optimal substitution with LN2 quenching are shown in Fig. 1.

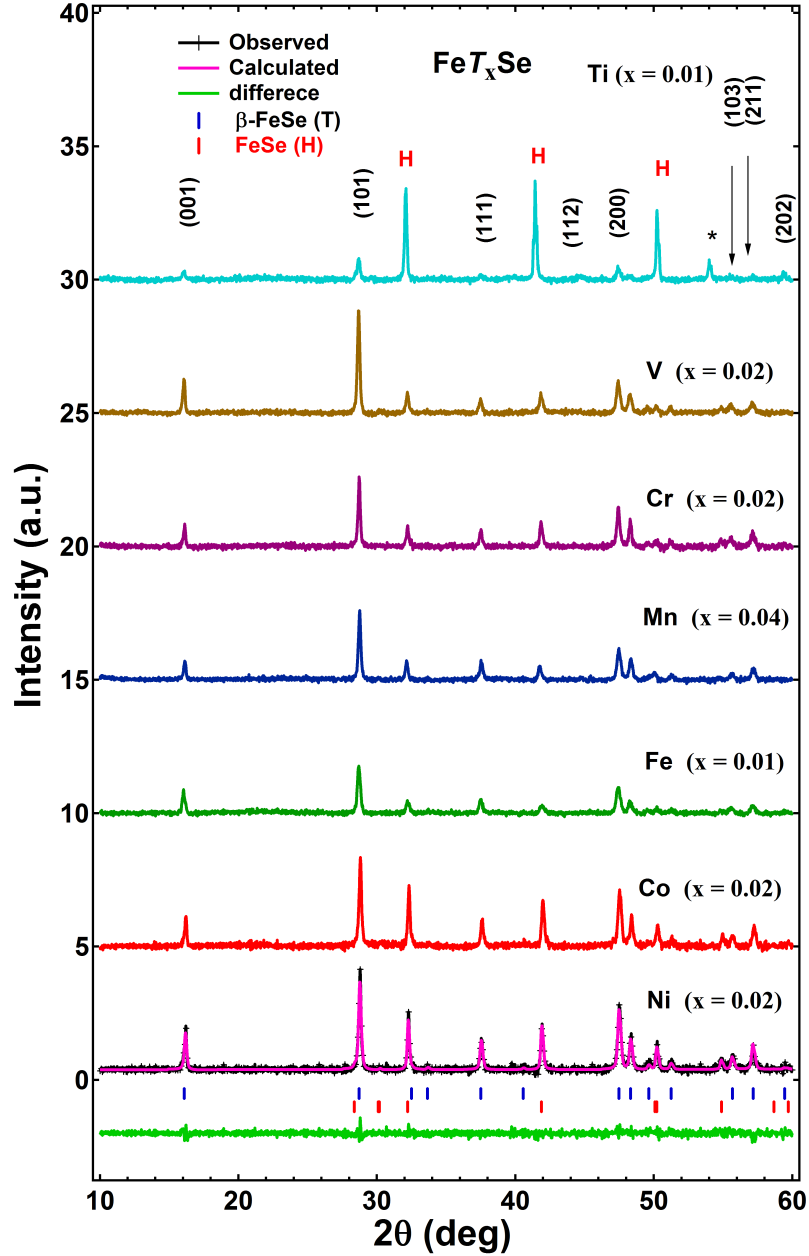


FIG. 1: (Color online) Powder X-ray diffraction patterns of all optimally doped FeT_xSe ($T = \text{Ni}, \text{Co}, \text{Fe}, \text{Mn}, \text{Cr}, \text{V}$ and Ti) samples. The XRD peaks which match with the tetragonal structure are indexed with (h, k, l) values and the peaks that match with the hexagonal structure are indicated with the symbol H. Asterisk denotes other impurity peaks.

The Rietveld refinements were performed for all the samples using the FullProf software. All the observed peaks could be indexed well only if two phases, the tetragonal β -FeSe ($P4/nmm$ space group) and the hexagonal α -FeSe ($P6_3/mmc$ space group), were included in the refinement. Result of one such a refinement is also shown in Fig. 1 for FeNi_{0.02}Se. The peaks which match with the tetragonal phase are indexed with the corresponding (h, k, l) values and the peaks that match with the hexagonal phase are marked with H in Fig. 1. However, if the peaks could not be indexed by either of the phases, then they are marked as impurity with an asterisk. Various parameters obtained from the refinements are given in Table I.

TABLE I: Lattice parameters obtained using the two phase (β -FeSe tetragonal phase and α -FeSe hexagonal phase) Rietveld refinements at 300 K from powder XRD data. β -FeSe belongs to the $P4/nmm$ space group with atomic positions: Fe: $2a(3/4, 1/4, 0)$, T: Ni, Co, Fe, Mn, Cr, V, Ti: $2a(3/4, 1/4, 0)$, Se: $2c(1/4, 1/4, z)$ and α -FeSe belongs to the $P6_3/mmc$ space group with atomic positions: Fe: $2a(0, 0, 0)$, Se: $2c(x, y, 1/4)$. The samples indicated with Q are quenched in LN2 from 360°C and the samples cooled in the natural way to room temperature are marked as RT.

| Compounds | a (Å) | c (Å) | c/a | V (Å ³) | Tet. (W%) | Hex.(W%) | T_c (K) |
|---------------------------------|---------------------|---------|-------|-----------------------|-----------|----------|-----------|
| FeNi _{0.02} Se (Q) | 3.774 | 5.519 | 1.462 | 78.61 | 64.1 | 35.9 | 0.0 |
| FeCo _{0.02} Se (Q) | 3.771 | 5.522 | 1.464 | 78.53 | 49.6 | 50.4 | 0.0 |
| Fe _{1.01} Se (RT) | 3.768 | 5.521 | 1.465 | 78.40 | 82.8 | 17.2 | 8.2 |
| Fe _{1.01} Se (Q) | 3.771 | 5.520 | 1.465 | 78.27 | 83.7 | 16.3 | 9 |
| FeMn _{0.04} Se (RT) | 3.770 | 5.522 | 1.464 | 78.49 | 86.1 | 13.9 | 10 |
| FeMn _{0.04} Se (Q) | 3.775 | 5.527 | 1.464 | 78.61 | 63.3 | 36.7 | 10 |
| FeCr _{0.02} Se(RT)[21] | 3.773 | 5.524 | 1.464 | 78.64 | 84.6 | 15.4 | 10.5 |
| FeCr _{0.02} Se(Q) | 3.767 | 5.519 | 1.465 | 78.31 | 50.1 | 49.9 | 11.0 |
| FeV _{0.02} Se(RT) | 3.772 | 5.524 | 1.464 | 78.62 | 82 | 18 | 9.5 |
| FeV _{0.02} Se(Q) | 3.772 | 5.520 | 1.463 | 78.56 | 78.5 | 21.5 | 11.2 |
| FeV _{0.03} Se(Q) | 3.776 | 5.508 | 1.463 | 78.01 | 10 | 90 | 9.2 |
| FeV _{0.05} Se(Q) | No tetragonal phase | | | | 0 | 100 | 0 |
| FeTi _{0.01} Se(RT) | 3.773 | 5.525 | 1.464 | 78.69 | 76.3 | 23.7 | 8 |
| FeTi _{0.01} Se(Q) | 3.770 | 5.518 | 1.463 | 78.43 | 15.1 | 84.9 | 11.0 |

The lattice parameters were found to be unaffected by the nominal substitution of the transition metal. It is not expected that such a small percentage of substitution by various transition metal ions will vary the lattice parameters significantly. We have confirmed the incorporation of the transition metals into the stoichiometry through the EDAX spectra for all the compositions (see Table II). The EDAX results are average value of composition that shows slight variation in stoichiometry. However stoichiometry from Rietveld refinement is very close to starting sto-

TABLE II: Composition from EDAX and Rietveld analysis of as grown FeT_xSe samples

| S. No. | Substituted element (T) | Starting composition | Average composition from EDAX | Rietveld refinement stoichiometry |
|--------|-----------------------------|-------------------------------|--|---|
| 1 | Ni | $\text{FeNi}_{0.02}\text{Se}$ | $\text{Fe}_{1.1}\text{Ni}_{0.02}\text{Se}_{0.9}$ | $\text{FeNi}_{0.02}\text{Se}$ |
| 2 | Co | $\text{FeCo}_{0.02}\text{Se}$ | $\text{Fe}_{0.98}\text{Co}_{0.02}\text{Se}_{0.82}$ | $\text{FeCo}_{0.02}\text{Se}$ |
| 3 | Fe | $\text{Fe}_{1.01}\text{Se}$ | $\text{Fe}_{1.02}\text{Se}_{0.96}$ | $\text{Fe}_{0.99}\text{Fe}_{0.01}\text{Se}$ |
| 4 | Mn | $\text{FeMn}_{0.04}\text{Se}$ | $\text{Fe}_{1.23}\text{Mn}_{0.05}\text{Se}_{0.98}$ | $\text{Fe}_{0.997}\text{Mn}_{0.04}\text{Se}$ |
| 5 | Cr | $\text{FeCr}_{0.02}\text{Se}$ | $\text{Fe}_{1.02}\text{Cr}_{0.02}\text{Se}_{0.9}$ | $\text{Fe}_{0.99}\text{Cr}_{0.02}\text{Se}$ |
| 6 | V | $\text{FeV}_{0.02}\text{Se}$ | $\text{Fe}_{0.95}\text{V}_{0.02}\text{Se}_{1.05}$ | $\text{Fe}_{0.99}\text{V}_{0.02}\text{Se}$ |
| 7 | Ti | $\text{FeTi}_{0.02}\text{Se}$ | $\text{Fe}_{0.99}\text{Ti}_{0.02}\text{Se}_{0.99}$ | $\text{Fe}_{0.997}\text{Ti}_{0.01}\text{Se}_{0.99}$ |

ichiometry of samples. A curious observation is the fact that the percentage of the hexagonal phase increases significantly in some cases (Mn and Ti) due to quenching, even though the quenching process was supposed to reduce the unwanted hexagonal phase.

B. Magnetization

Figures 2 (a)–(f) show the results of zero field-cooled (ZFC) and field-cooled (FC) dc magnetic susceptibility (χ_{dc}) for all the optimally doped transition metal-excess samples from 2 K to 13 K. Superconductivity as well as transition temperature (T_c) get suppressed in the Ni (2 wt %) and Co (2 wt %) excess samples (Fig. 2(a)). We see only a small dip in the magnetization in both the Ni- and Co-excess samples. Similar type of suppression of superconductivity was also observed by other groups with the doping of 1 wt% Ni and Co in FeSe [16, 17, 25]. Figure 2 (b) shows the $\chi_{\text{dc}}(T)$ measurements for the parent compound with excess Fe, but synthesized by the quenching process. There is only a slight change in T_c (~ 9 K) as compared to the T_c of the samples or the single crystals prepared in the usual way (slow cooling) [4, 24, 26, 27]. Samples with the substitution of excess iron more than 1 wt% were also prepared by the LN2 quenching method, but did not yield any enhancement in T_c . The $\chi_{\text{dc}}(T)$ data for the other transition metal substitutions are shown in Figs. 2 (c)–(f), where we observe an enhancement in T_c . The optimal substitution for the highest T_c and the shielding fraction varies for each transition metal element; Mn – 4 wt%, Cr – 2 wt%, V – 2 wt% and Ti – 1 wt%. The ac susceptibility measurement is usually used as a better tool for a more precise measurement of the T_c since the measurement can be performed without the application of any dc magnetic field [28]. The ac susceptibility measurement (in zero dc field) with temperature for all the substituted samples are plotted along with the dc magnetization in Figs. 2(b)–(f).

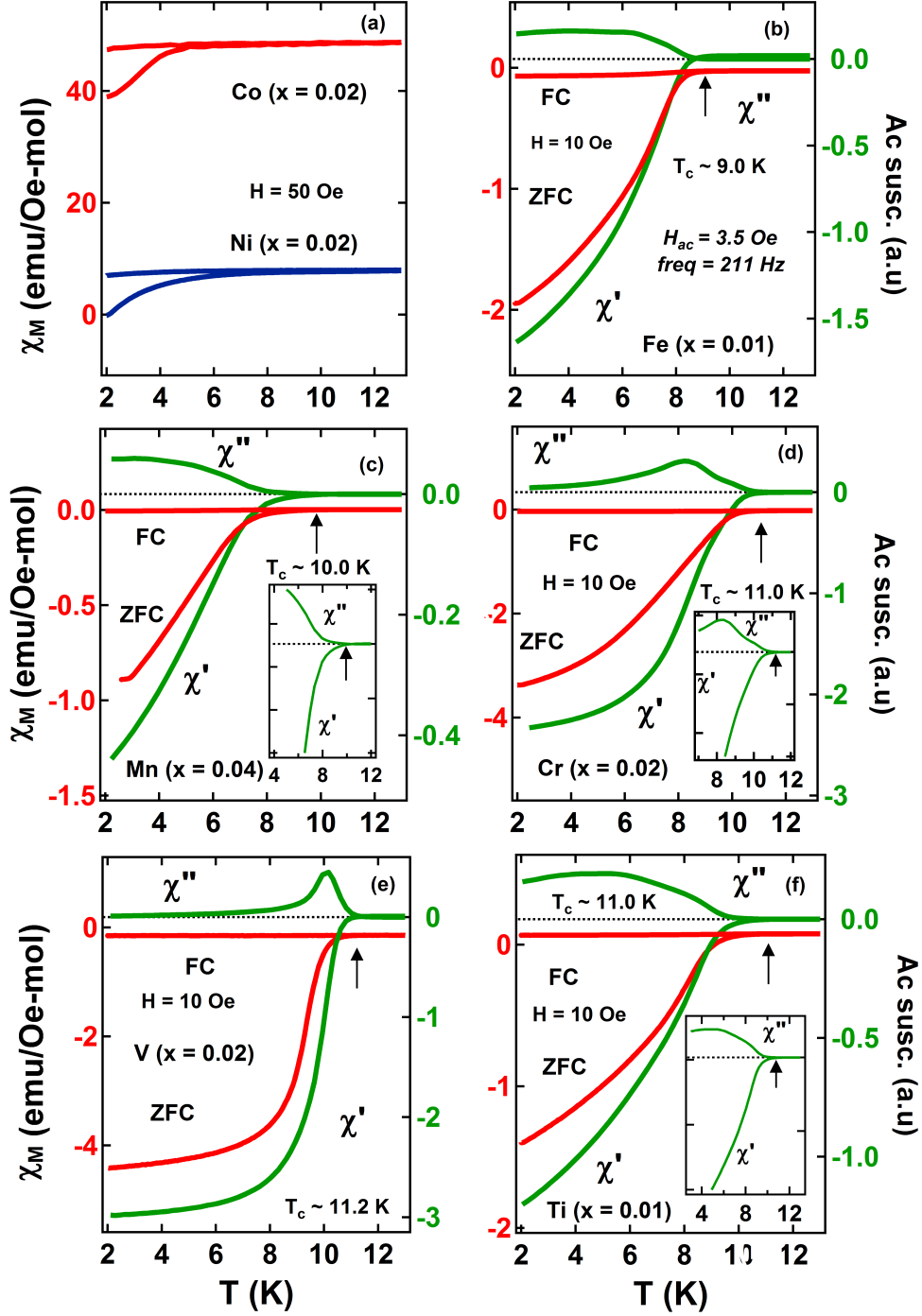


FIG. 2: (Color online) (a)-(f) Temperature dependence of zero field-cooled (ZFC) and field-cooled (FC) magnetization for all the optimally doped FeT_xSe samples (in red color; left axis). Temperature dependence of ac susceptibility (χ' and χ'') for the corresponding samples is shown in green color (right axis). Inset figures show the expand view of ac curves near T_c .

The transition temperatures are determined from the deviation of χ' (in phase with applying ac signal) and χ'' (out of phase) from the zero line, which are listed in Table I. The sharpness of the χ'' peak can be taken as the quality of the superconducting sample. Inset of Figs. 2(c),(d)

and (f) show the expand portion of ac susceptibility where the bifurcation start in χ' and χ'' to extract the T_c .

C. Electrical transport measurement

The main panel of Fig. 3(a) shows the temperature dependence of resistivity in zero field from 2 K to 300 K for all the optimally doped FeT_xSe compounds, except Ti (resistance for Ti-substituted sample could not be measured due to the brittle nature of the sample). The resistivity curves show typical 'S' shaped curvature in the full temperature range, which may be associated with the pseudo-gap at the Fermi surface in these compounds at higher temperatures [29]. The Fe-excess compound is found to have the highest resistivity among all the superconducting Fe_{1+x}Se compounds, while the non superconducting Ni-excess sample is found to have the largest resistivity amongst all the compounds. The metallic characteristic of these compounds were determined by calculating the residual resistance ratio ($\text{RRR} = \rho_{300\text{K}}/\rho_{15\text{K}}$) which is given in Table III. These values of RRR are smaller than the values for typical metallic conductors which suggests qualitatively that these compounds are relatively bad conductors. The behaviour of resistance near the transition temperature is highlighted in the inset of Fig. 3(a), where the expanded portion of the curves near the T_c are shown between 2 K to 20 K. Fig. 3(b) shows the typical resistivity curves at zero field and 90 kOe for $\text{FeV}_{0.02}\text{Se}$ in entire temperature range. The normal state resistance differs considerably from the zero field values when the magnetic field is applied, implying a large magneto-resistance in this compound. At about $\sim 73\text{K}$ the two resistivity curves cross-over (see inset of Fig. 3(b)) such that the resistivity which was higher for 90 kOe now becomes lower compared to the zero field resistivity. This crossing-over of the curves may be associated with the structural phase transition from the tetragonal to the orthorhombic phase observed in the low temperature XRD measurements of Fe_{1+x}Se compound [4, 10, 25].

Fig. 4(a) and (b) show the temperature dependent $\rho(T)$ curves at various fields ranges from 0 kOe to 90 kOe for $\text{Fe}_{1.01}\text{Se}$ and $\text{FeV}_{0.02}\text{Se}$. We have marked three transition temperatures, T_c^{on} , T_c^{mid} and T_c^{off} , which are defined as 90%, 50% and 10%, respectively, of the normal state resistivity at $T = 15\text{K}$. The upper critical field ($H_{c2}(T)$) plots, determined at these three transition temperatures for both samples are shown in insets of Fig. 4(a) and (b). Similar, estimation of $H_{c2}(T)$ values for all the other compounds were also done and the values for each superconducting sample are listed in Table III. The $H_{c2}(0)$ values were determined using the WHH formula [30], $H_{c2}(0) = -0.693T_c(dH_{c2}/dT)_{T_c}$, where $(dH_{c2}/dT)_{T_c}$ is the slope at the transition temperature and are given in table III (only for the mid transition temperature). The Mn substituted compound has the largest $H_{c2}(0)$ ($\sim 236\text{kOe}$) value whereas the other compounds

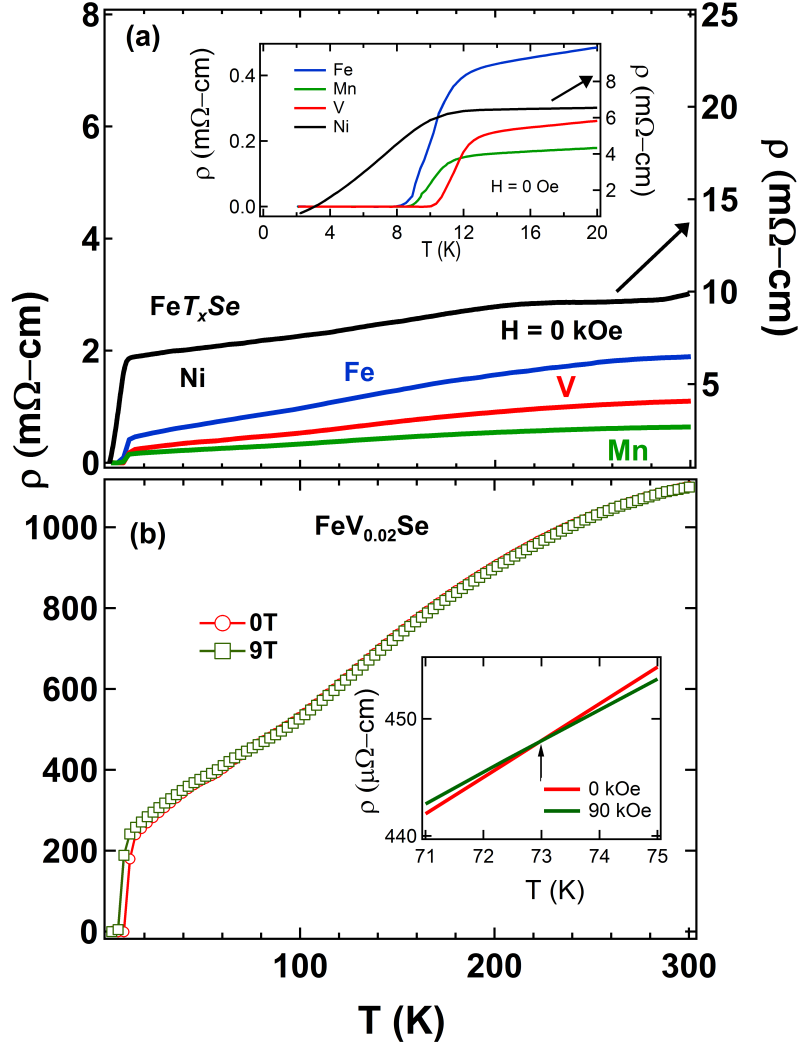


FIG. 3: (Color online) (a) Resistivity as function of temperature plots in zero field for FeT_xSe (Main panel). Inset shows the $\rho(T)$ curves from 2 K to 20 K. (b) shows $\rho(T)$ curves for $\text{FeV}_{0.02}\text{Se}$ at 0 kOe and 90 kOe from 2 K to 300 K. Inset shows the crossing of the zero and 90 kOe $\rho(T)$ curves (indicated by the arrow).

have comparable $H_{c2}(0)$ (~ 210 kOe) values. These $H_{c2}(0)$ values are comparable to the Pauli paramagnetic limit [31] of $H_p = 1.84T_c^{\text{mid}}$, which are also listed in Table III. This suggests that the spin-paramagnetic effect may be the dominant pair-breaking mechanism in FeT_xSe samples as reported for 'Fe-11' superconductors [9, 29, 32–34]. The superconducting coherence lengths ($\xi(0)$) were estimated using the Ginzburg-Landau formula $H_{c2}(0) = \phi_0/2\pi\xi^2$, which are listed in Table III. The $\xi(0)$ values for these substituted compounds are larger than the Te- [34] and S-substituted compounds [35].

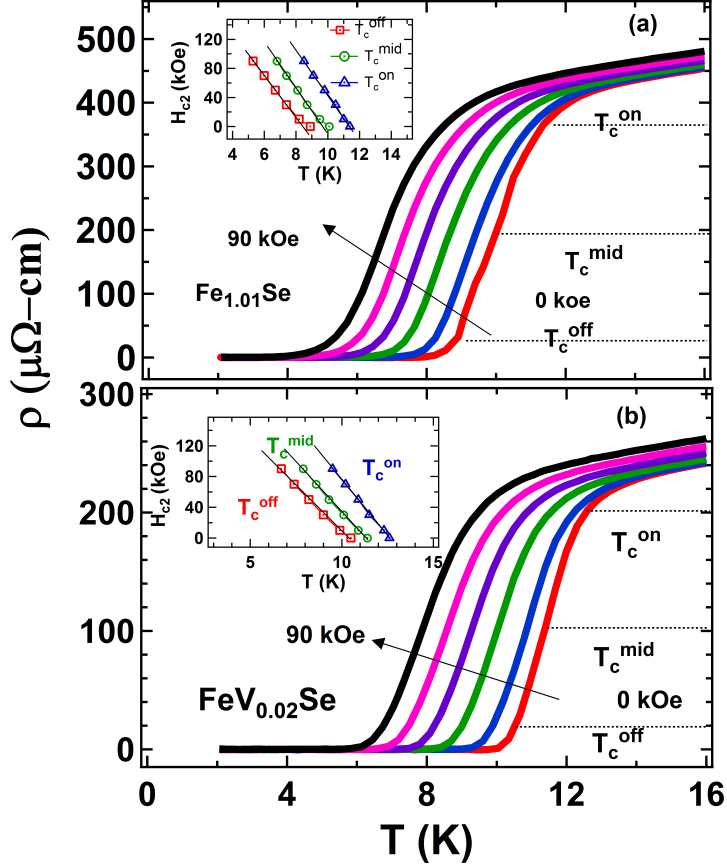


FIG. 4: (Color online)(a) and (b) Temperature dependent resistivity curves in presence of magnetic fields from 0 kOe to 90 kOe for $\text{Fe}_{1.01}\text{Se}$ and $\text{FeV}_{0.02}\text{Se}$ samples. Insets (a) and (b) show H_{c2} vs T phase diagram at three transition temperatures, T_c^{on} , T_c^{mid} and T_c^{off} (see text).

TABLE III: Superconducting parameters extracted from the electrical transport measurements

| Compound | T_c (K) | | | | | $H_{c2}^{\text{mid}}(0)$ (kOe) | $\xi(0)$ (nm) | $H_p^{\text{mid}}(0)$ (kOe) | H_{c1} (Oe) | RRR |
|-------------------------------|-------------------|--------------------|--------------------|-------------------|-------------------|-----------------------------------|------------------|--------------------------------|---------------|-----|
| | T_c^p | | | T_c^x | | | | | | |
| | T_c^{on} | T_c^{mid} | T_c^{off} | T_c^{dc} | T_c^{ac} | | | | | |
| $\text{Fe}_{1.01}\text{Se}$ | 11.4 | 10.1 | 8.9 | 8.9 | 9.0 | 210 | 3.96 | 185 | 9.5 | 4.1 |
| $\text{FeMn}_{0.04}\text{Se}$ | 11.2 | 10.1 | 9.2 | 9.8 | 10.0 | 236 | 3.73 | 185 | 10 | 3.9 |
| $\text{FeCr}_{0.02}\text{Se}$ | 13.2 | 12.0 | 11.0 | 10.9 | 11.0 | 222 | 3.98 | 220 | 24 | 8.1 |
| $\text{FeV}_{0.02}\text{Se}$ | 12.6 | 11.4 | 10.8 | 11.2 | 11.2 | 210 | 3.96 | 210 | 70 | 4.6 |

D. Thermal transport properties

Figure 5 shows the temperature dependence of thermal conductivity (κ) measured from 2 K to 300 K at zero field for $\text{Fe}T_x\text{Se}$ ($T = \text{Ni, Mn and V}$) samples.

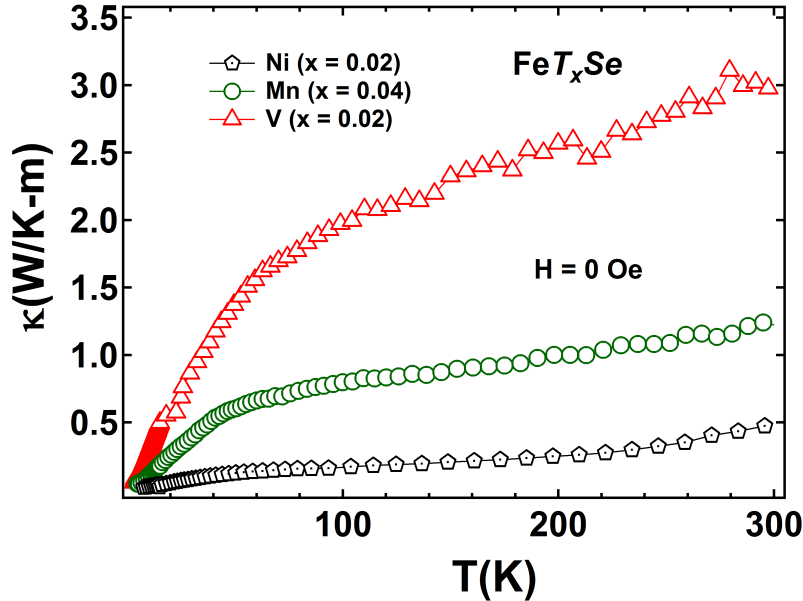


FIG. 5: Temperature dependence of thermal conductivity (κ) for FeT_xSe ($T = \text{Ni}, \text{Mn}$ and V) samples at zero field.

The κ is the highest for $\text{FeV}_{0.02}\text{Se}$ sample, which is almost six times larger than that of the lowest κ in $\text{FeNi}_{0.02}\text{Se}$, however all samples have comparatively lower κ compared to single crystal $\text{FeCr}_{0.02}\text{Se}$ [21]. If we correlate κ to the number of charge carriers, then the higher value of κ implies larger number of charge carriers as the lattice is the same for all these compounds. This indicates a correlation may exist qualitatively between the numbers of charge carriers and in the enhancement of T_c , if we compare the T_c (Table I) of these compounds which varies as $T_c^{\text{V}} > T_c^{\text{Mn}} > T_c^{\text{Fe}} > T_c^{\text{Ni}}$. On this basis charge carriers may also have a role in the enhancement of T_c in Fe-11 compounds, as in the case of iron pnictide superconductors [36, 37].

In Fig. 6(a), we have plotted the typical thermopower (S) behavior as a function of temperature for the FeT_xSe ($T = \text{Ni}, \text{Mn}$ and V) samples. The thermopower of all the compounds show an 'S' like curvature, typical of the Fe superconductors where $S(T)$ decreases with decreasing temperature and goes through a minimum between 70 K–180 K. It is reported that the thermopower of $\text{Fe}_{1.01}\text{Se}$ changes its sign from positive to negative at ~ 157 K and again from negative to positive at ~ 91 K [29]. Similar behaviour is seen only for the $\text{Fe}_{1.01}\text{Se}$ sample in our studies. We have observed a similar cross-over of S in our earlier studies where Cr was substituted as excess at the Fe site [21]. The changing of sign at ~ 93 K has been associated with a structural transition in $\text{Fe}_{1.01}\text{Se}$. Since the sign of thermopower (S) indicates the type of dominant charge carriers, one can argue that the compounds, $\text{Fe}_{1.01}\text{Se}$ and $\text{FeCr}_{0.02}\text{Se}$ [21], have both type of charge carriers where as the compounds, $\text{FeV}_{0.02}\text{Se}$, $\text{FeMn}_{0.02}\text{Se}$ and $\text{FeNi}_{0.02}\text{Se}$, have

only holes as major charge carriers since the sign of $S(T)$ is positive throughout the temperature range in these compounds.

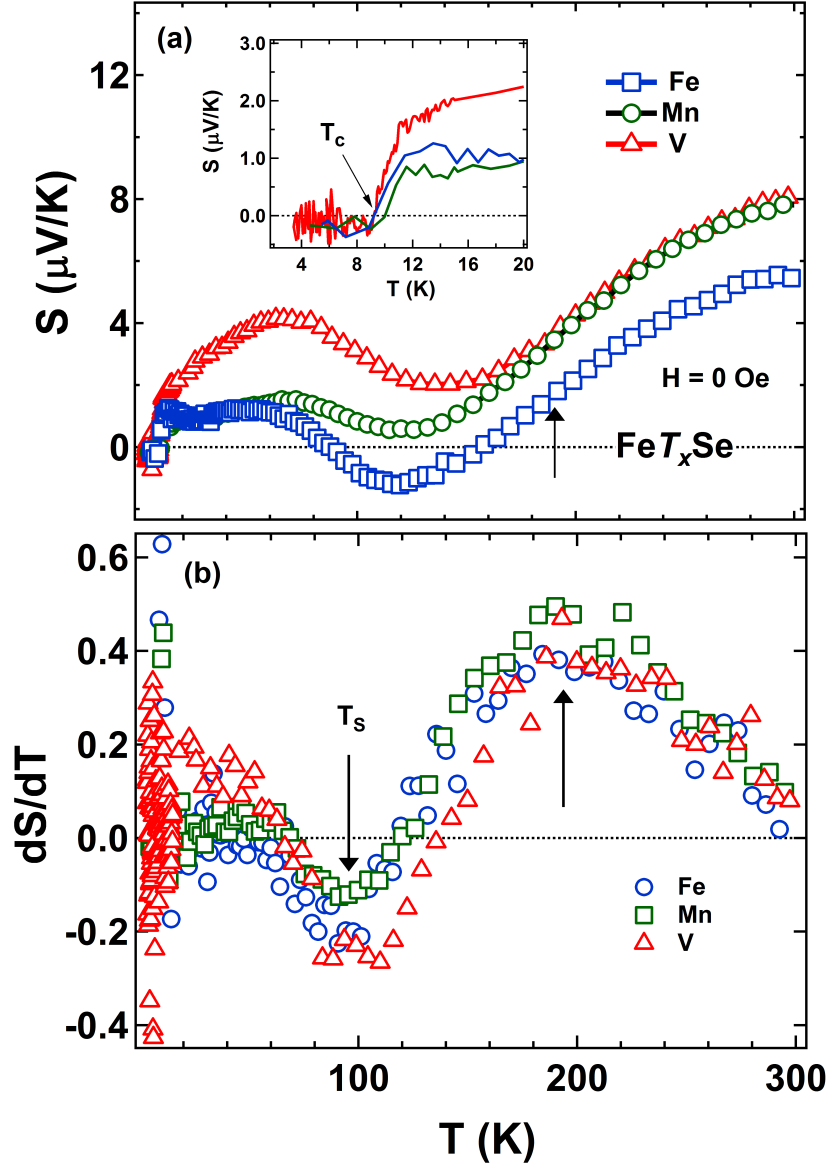


FIG. 6: (a) Temperature dependence of Seebeck coefficient (S) for FeT_xSe ($T = \text{Ni, Fe, Mn}$ and V). Inset shows the enlarged view of $S(T)$ between 2 K to 20 K and arrow indicates the T_c of compounds. (b) dS/dT vs T plots to highlight the similar behaviour of transitions in the three compounds (see text).

Inset of Fig. 6 (a) shows an enlarged view of $S(T)$ from 2 K to 20 K. In the superconducting state, the Seebeck coefficient becomes zero since the charge carriers have zero entropy as they are involved in the Cooper pair formation. As the temperature increases, the thermal energy overcomes the binding energy of the Cooper pairs and the superconductor gradually enters into the normal state as shown in the inset of Fig. 6 (a). Figure 6 (b) shows the derivative plots of $S(T)$ to highlight the similarity between compounds. Even though the Ni, V and Mn-substituted

samples did not show the cross-over to the negative values, their overall behavior is the same, as evident from the derivative plots. The modulation in derivative of $S(T)$ curves can be connect through previous studies on FeSe compounds. As it is seen in theoretical [38, 39] as well as experimental [40] studies, Fe-superconductors are semi-metal in nature and both types of charge carriers present at Fermi surface. Experimentally, we have also observed the presence of both types charge carriers in single crystals $\text{FeCr}_{0.02}\text{Se}$ [21]. The slops change at higher temperature for these FeT_xSe samples occur near same temperature (~ 200 K) where types of charge carriers change in Hall measurement for single crystal of $\text{FeCr}_{0.02}\text{Se}$ [21]. However, slop change at lower temperature ~ 93 K is associated with structural transition (tetragonal to orthorhombic) as previous reported in many references [4, 10, 24, 41].

IV. DISCUSSION

The quality of FeSe samples are always a concern and a subject of discussion since a variety of closely related phases like Fe_3O_4 , unreacted Fe, hexagonal FeSe, Fe_7Se_8 , etc., can form a part of the prepared samples. Many groups attempted to synthesis the pure tetragonal phase, but considerable amount of other impurities could not be avoided [26, 42]. As per the phase diagram studied by McQueen *et al.* [24], the formation of the hexagonal (non superconducting) phase occurs at temperatures below 200°C . In order to minimize this phase, we have quenched our samples from higher temperatures (360°C), but the percentage of hexagonal phase is found to increase. The interesting fact is that the impurity of hexagonal phase does not affect the T_c of the parent compound adversely; its presence is found to enhance the T_c in TM-substituted compounds (except Ni and Co). It is also found that the optimal substitution for the maximum T_c in each TM substituted compound is different (Fe – 1 wt%, Mn – 4 wt%, Cr – 2 wt%, V – 2 wt%, Ti – 1 wt%). Further substitution of TM beyond the optimal value is found to increase the hexagonal phase and decrease the tetragonal phase. The value of wt% substitution for the complete conversion into the hexagonal phase is different for different substitutions (Mn, Cr > 7 wt%, V ≥ 5 wt%, Ti ≥ 2 wt%). It looks as if the higher the ionic radius of the substituted TM metal, the less wt% of the dopant is required for the conversion into the complete hexagonal phase. It is also found that the T_c as well as the diamagnetic shielding fraction decreases with increasing hexagonal phase. As an example, we show in Fig. 7, the magnetic susceptibility data for the V-substituted samples (prepared by LN2 quenched method). The diamagnetic shielding fraction drastically gets decreased along with a decrease in T_c as the V-substitution increases beyond 2 wt%. For the V substitution beyond 5 wt% or more, the XRD patterns indicate the presence only the hexagonal phase (see Table I).

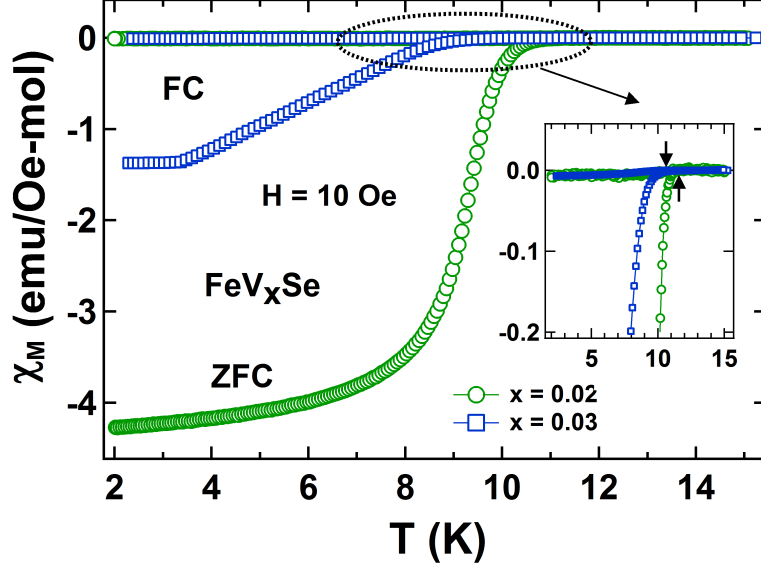


FIG. 7: Temperature dependence of zero field-cooled and field-cooled plots in 10 Oe for FeV_xSe ($x = 0.02, 0.03$). Inset figure shows the enlarge view of magnetization near transition.

The variation of T_c with atomic radius of the excess substituted transition metal in Fe_{1+x}Se is shown in Fig. 8. There is a clear indication that the T_c of the compound gets suppressed or destroyed when the transition metal with atomic radius less than that of Fe is substituted as excess, whereas the T_c gets enhanced when TM atoms with radius higher than the Fe atom are substituted. It is reported that the application of external pressure increases the T_c in FeSe compounds [11, 16]. If we correlate the increase in T_c in our substituted compounds, then we can assign a chemical pressure which will be equivalent to an external pressure of ~ 0.5 GPa [16]. If we compare the maximum T_c obtained for various TM metal substitutions (Fig. 8), we can bring in a correlation between the enhancement of T_c and the magnetic moment of the TM ion. T_c is found to increase as the moment decreases. The absence of superconductivity in Co and Ni substituted compounds may be associated with the dependence of ionic radius of the TM on the T_c . Since they have ionic radius less than that of the Fe, it is possible that they do not exert enough chemical pressure for the appearance of superconductivity. Thus we can conclude that all the three effects, the amount of hexagonal phase (chemical pressure), ionic radius and magnetic moment of the substituted TM, may play a role in the enhancement/suppression of T_c and hence the superconducting properties.

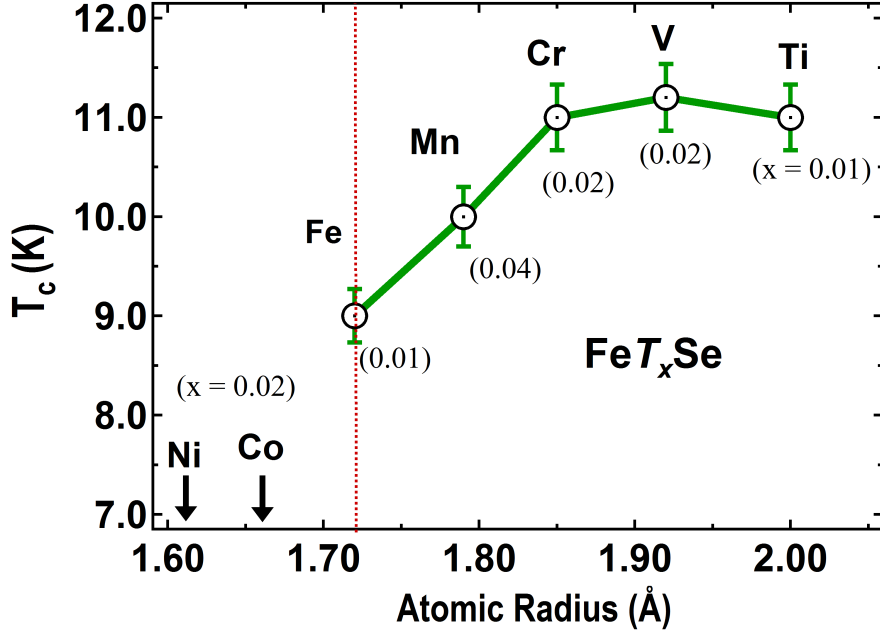


FIG. 8: Variation of T_c with atomic radius of the substituted transition metal ion in FeT_xSe compounds. The T_c of parent superconductor $\text{Fe}_{1.01}\text{Se}$, synthesis from quenching process, is shown by vertical dotted line.

V. CONCLUSIONS

We have studied the effect of nominal substitution of the transition metal ($T = \text{Ti}, \text{V}, \text{Cr}, \text{Mn}, \text{Fe}, \text{Co}$ and Ni) in place of excess Fe in Fe_{1+x}Se superconductor. All the FeT_xSe samples were synthesized successfully via a single step solid state reaction method, followed by quenching in LN2 from 360°C . All the presented transition metal (TM) substituted samples have tetragonal and hexagonal phases. The superconducting transition temperature is enhanced by 10% to 30% when TMs with higher ionic radius compared to that of the Fe is substituted. However, the substitution of the lower ionic radius TM suppresses the T_c . The optimal concentration for the highest T_c is found to be different for different TM substitutions. Both type of charge carriers were found to be present in the Fe- and Cr-excess samples, however, other TM substituted samples show positive sign of Seebeck coefficient throughout temperature range that indicates holes as majority charge carriers. In brief, we can conclude that the amount of hexagonal phase (chemical pressure), ionic radius as well as the magnetic moment of the substituted TM may play a role in the enhancement of T_c and hence the superconducting properties in the Fe-11 compound.

Acknowledgments

CVT would like to acknowledge the Department of Science and Technology for partial support through the project IR/S2/PU-10/2006. AKY would like to thank CSIR, India for SRF grant. ADT acknowledges the Indian Institute of Technology, Bombay for partial financial support during part of this work and the Indian Institute of Technology, Patna for seed grant.

- [1] Y. Kamihara, T. Watanabe, M. Hirano, and H. Hosono, *J. Am. Chem. Soc.* 130 (2008) 3296.
- [2] M. Rotter, M. Tegel, and D. Johrendt, *Phys. Rev. Lett.* 101 (2008)107006.
- [3] X. C. Wang, Q. Q. Liu, Y. X. Lv, W. B. Gao, X. L. Yang, R. C. Yu, F. Y. Li, and C. Q. Jin, *Solid State Commun.* 148 (2008) 538.
- [4] F. C. Hsu et al. *Proc. Natl Acad. Sci.* 105 (2008) 14262.
- [5] H. Ogino, Y. Matsumura, Y. Katsura, K. Ushiyama, S. Horii, K. Kishio, and J. I. Shimoyama, *Supercond. Sci. Technol.* 22 (2009) 075008.
- [6] W. Bao, Q. Huang, G. F. Chen, M. A. Green, D. M. Wang, J. B. He, X. Q. Wang, and Y. Qiu, *Chin. Phys. Lett.* 28 (2011a) 086104.
- [7] G. R. Stewart, *Rev. Mod. Phys.* 83 (2011) 1589.
- [8] C. Wang *et al.*, *Europhys. Lett.* 83 (2008) 67006.
- [9] Y. Mizuguchi *et al.*, *Appl. Phys. Lett.* 93 (2008) 152505.
- [10] S. Margadonna, Y. Takabayashi, Y. Ohishi, Y. Mizuguchi, Y. Takano, T. Kagayama, T. Nakagawa, M. Takata and K. Prassides, *Phys. Rev. B* 80 (2009) 064506.
- [11] S. Medvedev *et al.*, *Nature Mater.* 8 (2009) 630.
- [12] M. H. Fang, H. M. Pham, B. Qian, T. J. Liu, E. K. Vehstedt, Y. Liu, L. Spinu, and Z. Q. Mao, *Phys. Rev. B* 78 (2008) 224503.
- [13] K. W. Yeh, *et al.*, *Europhys. Lett.* 84 (2008) 37002.
- [14] B. C. Sales, A. S. Sefat, M. A. McGuire, R. Y. Jin and D. Mandrus, *Phys. Rev. B* 79 (2009) 094521.
- [15] T. Taen, Y. Tsuchiya, Y. Nakajima and T. Tamegai, *Phys. Rev. B* 80 (2009) 092502.
- [16] Y. Mizuguchi, F. Tomioka, S. Tsuda, T. Yamaguchi and Y. Takano, *J. Phys. Soc. Japan* 78 (2009) 074712.
- [17] M. K. Wu, *et al.*, *Physica C* 469 (2009) 340.
- [18] J. Guo, S. Jin, G. Wang, S. Wang, K. Zhu, T. Zhou, M. He, and X. Chen, *Phys. Rev. B* 82 (2010) 180520.
- [19] A. F. Wang *et al.*, *Phys. Rev. B* 83 (2011) 060512.
- [20] S. M. Kazakov, *et al.*, *Chem. Mater.* 23 (2011) 4311.
- [21] A. K. Yadav, A. D. Thakur and C. V. Tomy, *Phys. Rev. B* 87 (2013) 174524.
- [22] A. K. Yadav, A. D. Thakur, C. V. Tomy, *Solid State Commun.* 151 (2011) 557.
- [23] H. Okamoto, *J. Phase Equilib.* 12 (1991) 383.

- [24] T. M. McQueen *et al.*, Phys. Rev. B 79 (2009) 014522.
- [25] S. B. Zhang, H. C. Lei, X. D. Zhu, G. Li, B. S. Wang, L. J. Li, X. B. Zhu, W. H. Song, Z. R. Yang, Y. P. Sun, Physica C 469 (2009) 1958.
- [26] S. B. Zhang, *et al.*, Supercond. Sci. Technol. 22 (2009) 015020.
- [27] S. B. Zhang *et al.*, Supercond. Sci. Technol. 22 (2009) 075016.
- [28] R. H. Hein, Phys. Rev. B 33 (1986) 7539.
- [29] Y. J. Song, J. B. Hong, B. H. Min, K. J. Lee, M. H. Jung, J. S. Rhyee, Y. S. Kwon, J. Korean, Phys. Soc. 59 (2011) 312.
- [30] N. R. Werthamer, E. Helfand and P. C. Hohenberg, Phys. Rev. 147 (1966) 295.
- [31] A. M. Clogston, Phys. Rev. Lett. 9 (1962) 266.
- [32] G. F. Chen, Z. G. Chen, J. Dong, W. Z. Hu, G. Li, X. D. Zhang, P. Zheng, J. L. Luo and N. L. Wang, Phys. Rev. B 79 (2009) 140509.
- [33] S. Khim, J. W. Kim, E. S. Choi, Y. Bang, M. Nohara, H. Takagi, K. H. Kim, Phys. Rev. B. 81 (2010) 184511.
- [34] H. C. Lei, R. W. Hu, E. S. Choi, J. B. Warren and C. Petrovic, Phys. Rev. B 81 (2010) 184522.
- [35] Y. Mizuguchi, F. Tomioka, S. Tsuda, T. Yamaguchi, Y. Takano, Appl. Phys. Lett. 94 (2009) 012503.
- [36] X. Zhu, H. Yang, L. Fang, G. Mu, H. H. Wen, Supercond. Sci. Technol. 21 (2008) 105001.
- [37] H. H. Wen, G. Mu, L. Fang, H. Yang, X. Y. Zhu, Europhys. Lett. 82 (2008) 17009.
- [38] A. Subedi, L. Zhang, D. J. Singh, M. H. Du, Phys. Rev. B 78 (2008) 134514.
- [39] D. C. Johnston, Advances in Physics 6 (2010) 803.
- [40] Y. Xia, D. Qian, L. Wray, D. Hsieh, G. F. Chen, J. L. Luo, N. L. Wang, M. Z. Hasan, Phys. Rev. Lett. 103 (2009) 037002.
- [41] E. Pomjakushina, K. Conder, V. Pomjakushin, M. Bendele, R. Khasanov, Phys. Rev. B 80 (2009) 024517.
- [42] D. Braithwaite, B. Salce, G. Lapertot, F. Bourdarot, C. Marin, D. Aoki, M. Hanfland, J. Phys.: Condens. Matter 21 (2009) 232202.